Accepted Manuscript

The application of compound-specific sulfur isotopes to the oil–source rock correlation of Kurdistan petroleum

Paul F. Greenwood, Luma Mohammed, Kliti Grice, Malcolm McCulloch, Lorenz Schwark
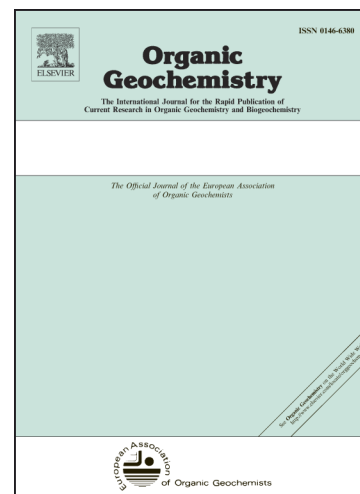
Please cite this article as: Greenwood, P.F., Mohammed, L., Grice, K., McCulloch, M., Schwark, L., The application of compound-specific sulfur isotopes to the oil–source rock correlation of Kurdistan petroleum, *Organic Geochemistry* (2017), doi: https://doi.org/10.1016/j.orggeochem.2017.11.016

The application of compound-specific sulfur isotopes to the oil–source rock

correlation of Kurdistan petroleum

Paul F. Greenwood [a,b*], Luma Mohammed [c], Kliti Grice [b], Malcolm McCulloch [a],

Lorenz Schwark [b,c]

[a] *Centre for Exploration Targeting and WA Biogeochemistry Centre, School of Earth*

Sciences, The University of Western Australia, M006, 35 Stirling Highway, Crawley,

WA 6009, Australia.

[b] *WA – Organic and Isotope Geochemistry Centre; and John de Laeter Centre, The*

Institute for Geoscience Research, Department of Chemistry, Faculty of Science and

Engineering, Curtin University, GPO Box U1987, Perth, WA 6845, Australia

[c] *Institute of Geoscience, Kiel University Ludewig-Meyn Str. 10, 24118 Kiel, Germany*

* corresponding author: paul.greenwood@uwa.edu.au

ABSTRACT

The concentrations and $\delta^{34}S$ values of thioaromatic compounds of a suite of oils from several major oil fields in Kurdistan and their corresponding regional Type II-S source rocks have been measured to investigate their source relationship. The oils of three fields (Khabbaz, Jambur, Ajeel) and the bitumen extracted from specific rock formations (Alan, Sargelu, Naokelekan, Chia Gara) showed particularly high abundances of thioaromatics consistent with a carbonate source deposited in a restricted sulfate-rich marine platform setting. The $\delta^{34}S$ [V-CDT] values of the major organosulfur compounds (OSCs) in these petroleum samples were measured with a gas chromatograph coupled to a multi-collector inductively coupled plasma mass spectrometer. $\delta^{34}S$ values of dibenzothiophenes and methyldibenzothiophenes were consistently in the range $-4‰$ to $-12‰$ and $-9‰$ to $-18‰$ for the oils and rocks, respectively. Separate groupings of oils and rocks were distinguishable by $> 2‰$ difference, given an analytical reproducibility of $< 0.8‰$. OSCs from rocks were consistently $\sim2–4‰$ depleted than in oils, reflecting a similar trend to previous bulk $\delta^{34}S$ studies from which an initial evolution of ^{34}S depleted H_2S during diagenesis and thermal maturation had been proposed. Distinctive $\delta^{34}S_{OSC}$ data of the oils and rocks with particularly high thioaromatic abundances did suggest several oils–source rock relationships: the Ajeel and Jambur oils and sediments from the Chia Gara formation yielded relatively enriched $\delta^{34}S_{OSC}$ values, whereas consistently depleted $\delta^{34}S_{OSC}$ values were observed for the Khabbaz oil and Naokelekan source rocks. Results

suggest that compound-specific S isotope analysis can help establish oil–source rock relationships of S-rich petroleum.

1. Introduction

The autonomous Kurdistan region of the Middle East is host to one of the world's largest active petroleum provinces. Exploration and field development in this region still affords tremendous oil exploration opportunities and continues to intensify.

Two major petroleum systems occur in Mesozoic strata: (1) the Middle–Upper Jurassic; and (2) the basal Cretaceous (Al-Ameri and Zumberge, 2012; Mohialdeen et al., 2013; Mohialdeen and Hakimi, 2016). Kurdistan oil fields in northern Iraq are located in the Zagros Fold Belt (of the Arabian platform), where the Jurassic and Cretaceous petroleum systems are generally well separated by the widespread carbonates/anhydrites of the Gotnia Formation. However, an absence of this unit or its replacement by the siliciclastic or brecciated Barsarin Formation can complicate the differentiation of the two petroleum systems and their respective contribution to many of the Kurdistan oils remains unclear.

Aliphatic terpenoid biomarkers indicative of deposition in Jurassic/Cretaceous shallow seas of the Arabian Carbonate Platform under restricted water circulation (e.g., high abundances of C_{28} $\alpha\beta$-hopane, 29,30-dinorhopane and extended hopanes, enrichment of the C_{24} tetracyclic terpenoid relative to tricyclics and low abundances of extended tricyclics) were recently reported in a suite of Kurdistan oils (Mohammed and Schwark, 2013). Strong anoxic/euxinic conditions were developed in basins with sulfur-rich marl to carbonate-anhydrite lithologies. Many of the oils had a high S content, being derived from Type II-S kerogens deposited in an anoxic, sulfur-rich

4

and iron-deficient depositional environment. The S-rich oils typically contained

relatively high abundances of OSCs, the distributions or $\delta^{34}S$ values of which may

help in supporting oil–source rock correlations, identify oil families or improve

oil–reservoir characterisation.

The $\delta^{34}S$ values of individual OSCs in oils or bitumen can now be measured

with gas chromatography combined with a multi-collector inductively coupled plasma

mass spectrometer (GC–ICPMS; Amrani et al., 2009). The $\delta^{34}S$ values of

thioaromatic and thioadamantane compounds have been measured in a range of oils of

different ages and petroleum provinces (Amrani et al., 2009, 2012; Greenwood et al.,

2014; 2015; Cai et al., 2015, 2016; Gvirtzman et al., 2015; Li et al., 2015; Ellis et al.,

2017). The $\delta^{34}S$ of the OSCs within and between oils can span a wide range, with

values as low as –21‰ detected in Smackover oils (Gulf of Mexico; Gvirtzman et al.,

2015) and > +40‰ in thermochemical sulfate reduction (TSR) impacted Tarim Basin

oils (NE China; Cai et al., 2015, 2016; Greenwood et al., 2015; Li et al., 2015). This

relatively large variance can be attributed to the variable sensitivity and isotopic

fractionation of different OSCs to the different S-processes impacting petroleum

systems, particularly TSR or microbial sulfate reduction (MSR), as well as potentially

petroleum migration or alteration (e.g., thermal maturation, water washing,

biodegradation). A slightly narrow range of $\delta^{34}S$ values measured from bulk oils (e.g.,

–8 to +32‰; Faure and Mensing, 2005) have proved useful for oil–oil correlations

(e.g., Gaffney et al., 1980; Thode, 1981; Orr, 1986; Cai et al., 2009a,b).

Here, we have measured the $\delta^{34}S$ values of organic sulfur compounds ($\delta^{34}S_{OSCs}$) in a suite of S-rich oils from several commercial Kurdistan oil fields and a series of potential source rocks, and integrated this with other traditional organic geochemical data, to help: (i) identify the major source rocks responsible for the Kurdistan oils; and (ii) investigate the relationship between the $\delta^{34}S$ values of OSCs from oils and source rocks.

Prospective mid Jurassic to lower Cretaceous source rocks of the Kurdistan oils occur in rock intervals of the Chia Gara (Upper Jurassic–Lower Cretaceous), Naokelekan (Upper Jurassic) and Sargelu (Middle Jurassic) formations (Dunnington, 2005; Al-Ameri et al., 2014; Mohialdeen and Hakimi, 2016), but their relative source significance has not been fully resolved. Hydrocarbon biomarkers including hopanoids (including gammacerane), steroids, and tricyclic terpenoids detected in Chia Gara rocks were consistent with largely marine algal and microbial inputs deposited in anoxic and saline stratified bottom waters (Mohammed, 2016; Mohialdeen and Hakimi, 2016). Hydrocarbon biomarkers have also revealed several source rock–oil reservoir relationships: e.g., high C_{27} diasterane abundances and elevated Ts/(Ts+Tm) ratios indicated that the Miocene reservoir units in the area were charged by the Jurassic petroleum system (Mohammed and Schwark, 2013). However, most of the rocks analysed in this study showed very similar terpenoid biomarker compositions, due to comparable depositional settings on a shallow carbonate platform, that limited a more detailed oil–source rock correlation.

The source rock–oil correlation potential of compound-specific sulfur isotope analysis (CSSIA) has not yet been fully established although in some recent studies the $\delta^{34}S_{OSC}$ data of: (i) several Tarim Basin oils (NW China) were correlated with Cambrian source rocks (Cai et al., 2015) – although the much speculated Cambrian or Ordovician source of the vast majority of Tarim Basin oils that have been analysed by GC–ICPMS (Cai et al. 2015, 2016; Li et al 2015) could not be distinguished due to complications such as mixing or alteration by thermochemical sulfate reduction (TSR); and (ii) bitumen produced by the pyrolysis of Ghareb Formation rock was correlated with adjacent Late Cretaceous organic chalk sourced oils (e.g., Gurim, Emuna; Rosenberg et al., 2017).

2. Methods

2.1. Geological setting

2.1.1. Stratigraphy and lithology of potential source rock and oil accumulations

Sedimentary rocks deposited on the Arabian Platform during the Late Jurassic to Early Cretaceous comprise carbonate and anhydrite minerals and carbonaceous shales, which accumulated organic matter deposited under anoxic and sulfur-enriched conditions (Dunnington, 2005; Mohialdeen and Hakimi, 2016). Low iron concentrations during deposition led to the organic incorporation of reduced sulfur into Type II-S kerogens. The stratigraphy of the Jurassic/Cretaceous formations of the study area with source potential is indicated in Fig. 1.

Increases in the thermal maturity of sediments upon formation of the Zagros

Fold Belt led to the generation and accumulation of large oil reservoirs, including the

giant Kirkuk field. A map of the Kurdistan oil province and major oil fields is given in

Fig. 2.

2.1.2. Source rocks stratigraphy and potential

Source rocks recovered from the Ajeel-12 well covering the time interval from

the Lower Middle Jurassic (Aalenian) to the Early Cretaceous (Barremian), were

made available from a previous study (Mohammed and Schwark, 2013; Mohammed,

2016). Prior high resolution (117 samples) Rock-Eval (RE) pyrolysis of Ajeel-12

rocks was acquired for a detailed appraisal of the petroleum generating potential of

the Jurassic–Cretaceous strata and selected data is included in Fig. 1. High TOC and

HI values, combined with T_{max} values largely within the oil window identified

substantial source rock potential in Sargelu, Naokelekan and Chia Gara Formations,

with possible further potential in transitional zones of the evaporitic Gotnia Formation

(Fig. 1). A suite of 18 rock samples (Table 1) covering the six main formations of

Ajeel-12 well were selected for the current CSSIA study.

2.1.3. Kurdistan production oils

A total of 29 production oils (Table 2) from the Kirkuk supergiant oil field and

the adjacent south-west oil fields of Bai Hassan, Khabbaz, Jambur, Hamrin, Ajeel,

Tikrit and Baji were analysed. These oils were all produced from Miocene (Euphrates,

Jeribe), Oligocene (Baba) and Eocene (Khurmala) reservoirs and largely charged

from Jurassic petroleum systems.

2.1.4. Sample preparation, GC–MS and CSSIA

Mono- and polyaromatic fractions of all oils and aromatic fractions of the rock

samples were made available from a previous study (Mohammed and Schwark, 2013;

Mohammed, 2016). Briefly, bitumen had been recovered from potential source rocks

by accelerated solvent extraction (DIONEX ASE-200) applying an azeotropic mixture

(93:7) of dichloromethane (DCM) and methanol (MeOH) at 50 bars and 75 °C over a

static phase of 25 min. Before further compound class separation, elemental sulfur

from extracts and oils was removed by adding activated copper. Oils and bitumen

extracts were separated into aliphatic, mono- and polyaromatic, or NSO fractions by

automated SPE using an LC-TECH Freestyle robot. Activated silica (2.8 g, 25–40 μm)

was dry filled into 8 ml SPE columns and overlain with 20 mg of oil/extract sorbed

onto a minimum amount of silica gel. Aliphatic hydrocarbons were eluted with 7 ml

of *n*-hexane, monoaromatics with a further 3 ml of hexane, polyaromatic

hydrocarbons with 6 ml hexane/dichloromethane (3:2, v:v) and NSO compounds were

eluted with 12 ml of DCM:MeOH (1:1, v:v). GC–MS measurements were performed

on an Agilent 5975B MSD interfaced to an Agilent 7890A gas chromatograph (GC)

equipped with a DB-5MS capillary column (30 m length, 0.25 mm i.d., 0.25 μm film

thickness). The temperature program used was: 70 °C (5 min isothermal) to 140 °C at

10 °C/min, then to 325 °C at 2 °C/min (held for 10 min). The quadrupole mass

spectrometer was operated in scan mode in the m/z 50 to 550 range. Compounds presented and discussed here (Pr, Ph, n-C_{17}, n-C_{18}, dibenzothiophenes/phenanthrene and methylated analogues) were identified via characteristic mass spectra and relative retention times, and peak areas, used to calculate product ratios, were integrated using the GC–MSD ChemStation Software (Agilent Technologies).

It was anticipated the thioaromatics (TAs) would concentrate in the polyaromatic fraction, but this was found not to be the case for all samples. Consequently, the mono- or polyaromatic fraction of each sample which showed the highest GC–MS concentration of thioaromatics was used for GC–ICPMS analysis. Analysis of OSCs common to the mono- and polyaromatic fractions of selected samples showed negligible $\delta^{34}S$ variance (< 1‰), indicating no obvious ^{34}S fractionation between these two sub-fractions.

The $\delta^{34}S$ values of OSCs in the mono- or polyaromatic fractions of the oils and rocks were measured with a Thermo Neptune Plus multi-collector ICPMS coupled to an Agilent 6890 GC inlet system (GC–ICPMS; Greenwood et al., 2015). The GC was fitted with a DB-5 capillary column (30 m × 0.25 mm i.d. × 0.1 μm film thickness). The oven was temperature programmed to increase from 80 °C (held 0.5 min) to 280 °C at 8 °C/min and He carrier gas was used at a rate of 5 ml/min. Pulses of SF_6 reference gas (−8.6‰) were introduced at the beginning and end of each GC run to facilitate the anchor point $\delta^{34}S$ calibration of the acquired data.

The m/z 32 (^{32}S) and m/z 34 (^{34}S) ICPMS ion currents were acquired in 131 ms increments by the Neptune software and exported to Excel in ASCII format. Peak

10

areas from background subtracted signals were manually processed in Excel to obtain the $^{34}S/^{32}S$ analyte ratios (Ra) used to calculate $\delta^{34}S$ values:

$\delta^{34}S = Ra/(Rs-1)$, where $Rs = {}^{34}S/^{32}S$ Standard (Vienna Canyon Diablo Troilite = 0.044151)

The ICPMS-measured $\delta^{34}S$ values were converted to true $\delta^{34}S$ with a normalisation curve established from the measurement of authentic standards of known $\delta^{34}S$ values (benzothiophene (BT) = +4.5‰; dibenzothiophene (DBT) = +13.7‰; 1-dodecanthiol ($C_{12}SH$) = −7.1‰; 1-octadecaenthiol ($C_{18}SH$) = +13.7‰) measured by Elemental Analysis isotope ratio mass spectrometry calibrated for $\delta^{34}S$ measurements with international standards provided by IAEA (IAEA-S1, IAEA-S2, IAEA-S3 and NBS127). External standards were also analysed daily to confirm the accuracy of the ICPMS measurements (precision typically < 0.5%). The $\delta^{34}S$ values reported for the OSCs of all samples are the mean of at least duplicate GC–ICPMS measurement typically with standard deviation values typically < 0.8‰, but larger for products of low concentration or those that were only partially GC resolved (i.e., some dimethylated and trimethylated DBT isomers).

Methyl DBT isomers were identified from previously reported GC elution data (Garcia et al., 2002). Isomeric identification of higher molecular weight alkyl DBTs (and alkyl BTs) was not attempted and these analytes are simply referred to as isomers i, ii or iii (i.e., $\delta^{34}S$ data was measured for up to 3 different isomers of some OSCs).

3. Results

11

3.1. Thioaromatic composition of oils and rocks

The *m/z* 32 chromatogram from GC–ICPMS analysis of the polyaromatic fractions of Ajeel oil sample 4407 and rock sample 4272 from the Chia Gara formation are shown in Fig. 3. The most abundant OSCs were alkyl-DBTs, whilst several alkyl-BTs were also evident. These thioaromatic profiles were generally representative of all the oils and rocks analysed although alkyl BTs were often absent or present in low concentrations presumably due to evaporative losses during sample preparation.

Several oils (Khabbaz, Jambur, Ajeel) and rock formations (Alan, Sargelu, Naokelekan, Chia Gara) showed particularly high abundances of thioaromatics consistent with a carbonate source deposited in sulfate-rich marine lacustrine setting. Other less S-rich oils (i.e., Bai Hassan, some Kirkuk) may have originated from mixed carbonate and shale sources deposited in a sulfate deficient environment.

3.2. δ^{34}S of thioaromatics in oils and rocks

δ^{34}S values were measured for the most abundant OSCs in the oils and rock extracts. This consistently included DBT and the first (4-) and co-eluting (2/3-) methyl DBT peaks, three dimethyl DBT peaks (i, ii, iii) and an early eluting trimethyl DBT peak (i). The δ^{34}S value of other OSCs could be measured for some samples (e.g., 1-methyl DBT in several oils and rocks and alkyl BTs in most of the oils and a few rocks), but their low concentrations in many samples limited these data so they have been excluded from the detailed δ^{34}S oil source rock assessment.

12

The $\delta^{34}S$ values measured for the OSC in the production oils ranged from −12‰ to +3‰ (Table 2) and in the rocks from −18‰ to −3‰ (Table 1). The rocks showed consistently depleted $\delta^{34}S_{OSC}$ values than the oils.

The OSCs within a given sample had very similar $\delta^{34}S$ values apart from a common depletion of a few ‰ with increasing methylation and molecular weight. There was relatively little variance in the data from specific production fields or rock formations. These data trends were evident from the $\delta^{34}S_{OSC}$ profiles of oil samples shown in Fig. 4. Production oil data, representing the averaged value from all oils of a given field, are compared in Fig 4a and $\delta^{34}S_{OSC}$ data of the three Jambur oils and the five Khabbaz oils are separately shown in Fig. 4b. The $\delta^{34}S_{OSC}$ values of the Jambur oils were consistently heavier than the Khabbaz oils (Fig. 4b), and the average $\delta^{34}S_{OSC}$ values within each of these two field spanned a range of ~3‰ (Fig 4a).

4. Discussion

4.1. $\delta^{34}S$ character of oils and rocks

The $\delta^{34}S$ values of the BTs and DBTs of the production oils varied from −12‰ to +3‰, with individual compounds showing very narrow value ranges. These values were similar to the −3.5‰ to −8.8‰ bulk $\delta^{34}S$ data of oils from several Kurdistan fields, including Jambur, Khabbaz and Bai Hussain, measured several decades ago (Thode and Munster, 1970) and considered remarkably close due to common Jurassic sources. The slightly larger range in the presently measured $\delta^{34}S_{OSC}$ may reflect the varied sensitivity of different OSCs to elements of the S-cycle of petroleum systems.

Alternatively, the oils may derive from two or more isotopically distinct sources to which different OSCs have a varied sensitivity. The unique source responses of compounds may be obscured by bulk $\delta^{34}S$ analyses. The bulk $\delta^{34}S$ analysis of kerogens or rocks might also be compromised by the persistence of inorganic sulfur species, such as pyrite which when finely dispersed in kerogen is difficult to fully remove by chemical treatment (Cai et al., 2009). This problem is avoided with the analyses of GC separated OSCs, although the solvent-extractable (i.e., bitumen) fractions of rocks analysed here might represent a quantitatively minor, and potentially isotopically unique, pool of organic S present in these samples.

The $\delta^{34}S$ values for the presently measured OSCs and previously of bulk oils previously are close to $-5‰$ which represents an approximate $20‰$ depletion from Jurassic–Cretaceous seawater sulfate values predicted from the analysis of sulfate minerals (Thode and Munster, 1970; Wu et al., 2014). This difference suggests minimal impact from TSR which would be expected to produce OSCs approaching the heavier $\delta^{34}S$ of mineral SO_4^{2-} sources (Amrani et al., 2012). Kurdistan oils have generally shown little evidence of TSR and the modest thermal maturity of the present oil suite (C_{29} $\beta\beta/(\beta\beta+\alpha\alpha)$ sterane ~ 0.54) suggests the high temperatures necessary to support TSR may not have been reached. Amrani et al. (2012) demonstrated the varied TSR stability and $\delta^{34}S$ sensitivity of BTs and DBTs and proposed that the $\delta^{34}S$ differential between these thioaromatic groups can often be a sensitive indicator of the early stages of TSR. There was a small but discernible distinction between $\delta^{34}S_{DBT}$ and more limited $\delta^{34}S_{BT}$ values of the rocks (Table 1) and oils (Table 2): The

14

$\delta^{34}S_{BT-DBT}$ of the oils was ~4‰ and for the rocks the difference was slightly higher at

~8‰. The moderate magnitude of these $\delta^{34}S_{BT-DBT}$ values is not indicative of the

occurrence of TSR. A recent CSSIA study of a suite of Bighorn Basin oils impacted to

varying degrees by TSR was unable to attribute a TSR impact to oils with $\delta^{34}S_{BT-DBT} \leq$

6‰ (Ellis et al., 2017). It was intriguing to note the consistently greater $\delta^{34}S_{BT-DBT}$

values (by few ‰) of the Kurdistan rocks compared to the Kurdistan oils. Under

favorable conditions TSR may occur in situ within rocks, but other factors (e.g.,

thermal maturity; Ellis et al., 2017) can also contribute to $\delta^{34}S$ differences between

BTs and DBTs.

The average oil field $\delta^{34}S$ values of DBT and specific alky DBTs reflected a

variance of ~4‰ between oil fields with enriched to depleted being: Jambur~Ajeel >

Hamrin > Kirkuk ~ Bai Hassan > Khabbaz (Fig. 4a). $\delta^{34}S_{OSC}$ differences between

samples is not likely due to thermal maturity since all of the oils studied were of

similar maturity, based on consistent C_{29} $\beta\beta/(\beta\beta+\alpha\alpha)$ sterane values (0.54 ± 0.03).

Very narrow $\delta^{34}S_{OSC}$ ranges were measured for the production oils of a given field.

The Khabbaz oil showed the largest variance of ~4‰ for most OSCs (Fig. 4b). Thode

and Monster (1970) also reported negligible differences in $\delta^{34}S$ values of oils from the

same field, even for a range of ages, but did note a small variation in $\delta^{34}S$ of similarly

aged oils of different fields. Local conditions (e.g., SO_4^{2-} and organic reactant

concentrations, temperature) can affect metabolic rates and the degree of isotopic

fractionation associated with microbial sulfate reduction. The organic incorporation of

reduced sulfur species is also typically associated with a small isotopic fractionation

15

(usually an enrichment; e.g., Amrani and Aizenshtat, 2004), which can vary for different diagenetic pathways. The $\delta^{34}S$ of the organic sulfur in petroleum can be subsequently influenced by thermal maturity (Ellis et al., 2017; Rosenberg et al., 2017) as well as potentially by other common geophysical or chemical impacts on petroleum.

The $\delta^{34}S_{OSC}$ profiles of all of the rock extracts were also generally similar, although an up to 8‰ range in values was evident within some formations (e.g., Gotnia). The span in $\delta^{34}S_{OSC}$ values of Chia Gara was 6‰ and for Naokelekan it was 4‰ (Table 1).

A plot of the $\delta^{34}S$ value of the first eluting methyl DBT and dimethyl DBT isomers for all oils and rocks is shown in Fig. 5. These were typically the most abundant isomers and gave the most precise $\delta^{34}S$ values (std. dev. < 0.6, i.e. smaller than the size of data points given in Fig. 5).

This consideration of just two of the available $\delta^{34}S$ values provided a good separation of most oil fields and rock formations demonstrating the sample correlation capacity of CSSIA. For example, the Khabbaz oils generally had the most depleted $\delta^{34}S$ values of the oils, and the Ajeel and Jambur oils generally the most enriched. Of the rocks, Chia Gara samples (apart from rock 4271) were heaviest and generally ~2–4‰ more enriched in ^{34}S than the Naokelekan extracts.

The enriched nature of the $\delta^{34}S_{OSC}$ values of the rock extracts (vs oils) is also clearly evident in Fig. 5. A similar trend has been reported from bulk $\delta^{34}S$ analysis of oils and source rocks. Monterey oils were reported to be 2‰ enriched than the

16

kerogen of their source rocks (Orr, 1986), and the oil expelled from laboratory conducted pyrolysis of immature kerogen showed a similar ^{34}S enrichment compared to the residual kerogen (Idiz et al., 1990; Amrani et al., 2005). These trends were attributed to the initial release of ^{34}S depleted H_2S on the thermal cracking of S–S and C–S kerogen bonds. This leads to residual kerogen being slightly enriched in ^{34}S from which oil was subsequently expelled at higher maturity. Alternatively, ^{34}S depleted H_2S might be formed via the secondary cracking of higher MW OSCs in the bitumen, as was suggested to account for ^{34}S enriched OSCs produced by the hydrogen pyrolysis (HyPy) treatment of several S-rich kerogens (Grotheer et al., 2017). S isotopic trends evident from a simulated thermal maturity study of Type II-S source rocks (Rosenberg et al., 2017) included the evolution of H_2S that was a few ‰ depleted in δ^{34}S than the immature kerogen, consistent with a kinetic control favouring release of ^{32}S, although the residual kerogen and oil released showed only a minor ^{34}S enrichment (δ^{34}S increase of +0.4‰). Furthermore, the kerogen S and oil phase OSCs showed a δ^{34}S homogenisation with increasing thermal maturity due to formation of new products from multiple S sources, thus becoming more reflective of the δ^{34}S of the bulk kerogen (Rosenberg et al., 2017).

4.2. Correlation of oils and rocks

The depositional environments and lithologies of petroleum source rocks can be inferred from a plot of DBT/phenanthrene (P) vs Pr/Ph (Hughes et al., 1995). These plots for the production oils and source rocks are shown in Fig. 6.

17

The production oils show two separate groupings in zones 1b and 2 as defined by Hughes et al. (1990), whereas most of the rocks plot in Zone 1b. Zone 1b is indicative of a carbonate or mixed source deposited in a sulfate-rich marine or lacustrine setting, whereas Zone 2 petroleum could derive from a number of possible sources deposited in a less sulfate-rich environment (Hughes et al., 1995). All of the Bai Hassan oils and several of the Kirkuk oils were categorised as moderate sulfate Zone 2 oils. The DBT/P and methyl DBT/methyl P plot (Fig. 6b; ratio values given in Table 2) provides a quite distinctive separation of these oils on the basis of their OSC content and reiterates the lower S content of the Bai Hassan oils. There was less resolution, however, of the other production oils. A subgroup of the Kirkuk oils and one Hamrin oil were also distinguished as being S-poor. All of the Ajeel, Khabbaz and Jambur oils, and all but a few rocks, gave relatively high abundance of thioaromatic compounds.

Triterpenoid biomarker profiles from GC–MS of the saturate fractions of three potential source units were previously shown to match well with the Ajeel and Hamrin oils (Mohammed and Schwark, 2013; Mohammed, 2016). This correlation included a consistently low abundance of tri- vs pentacyclic terpanes, a predominance of the C_{29} hopanes, the presence of 2-methylhopane but no gammacerane, and the peculiar occurrence of a 29,30-dinorhopane.

Sample resolution can be enhanced by considering a combination of $\delta^{34}S$ data from CSSIA and molecular data from GC–MS. This is demonstrated by plotting the $\delta^{34}S$ value of the first eluting dimethyl DBT ($\delta^{34}S_{dmDBTi}$) vs the DBT/P ratio of the

production oils (Fig. 7). The $\delta^{34}S_{dmDBTi}$ data help to resolve some of the S-rich oils, specifically distinguishing several of the Khabbaz oils from the Jambur, Ajeel and Kirkuk oils that had similar thioaromatic concentrations (e.g., Fig. 6b).

Several oils (Khabbaz, Ajeel and Jambur) and rocks (Chia Gara and Naokelekan) all plotted in Zone 1b (Fig. 6) consistent with a close molecular correlation, and potential oil–source rock relationship. $\delta^{34}S$ data may extend this correlation and help resolve further the contribution of the Chia Gara and Naokelekan rocks to these oil fields.

The $\delta^{34}S$ values of DBT and the first eluting of the methyl-, dimethyl- and trimethyl-DBTs for these three oils and two rocks are shown in Fig. 8. The Jambur and Ajeel oil showed almost identical $\delta^{34}S_{OSC}$ data and were consistently 2‰ enriched than the OSCs of the Khabbaz oil. The OSCs in Chia Gara rocks were similarly enriched by 3‰ compared to those in the Naokelekan rock. These trends suggest a greater OSC contribution of the S-isotopically enriched Chia Gara rocks to the enriched Jambur and Ajeel oils, and likewise the S-isotopically depleted Naokelekan rocks may have been more significant for the depleted Khabbaz oils.

19

4. Conclusions

The incorporation of $\delta^{34}S_{OSC}$ data measured by CSSIA with traditional molecular S indicators (e.g., DBT/P, methyl DBT/methyl P) enhanced the distinction of hydrocarbons from different Kurdistan oil fields and demonstrated how CSSIA can assist the organic geochemical characterization of S-rich oils. The OSCs extracted from rock formations thought responsible for large Kurdistan oil reservoirs were consistently ^{34}S depleted compared to the oils, making direct $\delta^{34}S$ correlations difficult. Nevertheless, similar trends such as relatively ^{34}S enriched oils and rocks allowed several potential relationships to be inferred. For instance, isotopically depleted OSCs from Ajeel and Jambur oils may have received a major contribution from Chia Gara rocks given the notable ^{32}S depletion of its products, and conversely relatively enriched $\delta^{34}S_{OSC}$ data suggest the Khabbaz oils may be predominantly sourced from Naokelekan rocks. The veracity of these inferences drawn here will need to be assessed by further CSSIA studies of oils and rocks.

20

Associate Editor–**Philippe Schaefer**

References

Al-Ameri, T.K., Zumberge, J., 2012. Middle and Upper Jurassic hydrocarbon
potential of the Zagross Fold Belt, North Iraq. Marine Petroleum Geology 36,
13–34.

Al-Ameri, T.K., Najaf, A.A., Al-Khafaji, A.S., Zumberge, J., Pitman, J., 2014.
Hydrocarbon potential of the Sargelu Formation, North Iraq. Arabian Journal of
Geosciences 7, 987–1000

Amrani, A., Aizenshtat, Z., 2004. Mechanisms of sulfur introduction chemically
controlled: δ^{34}S imprint. Organic Geochemistry 35, 1319–1336.

Amrani, A., Lewan, M.D., Aizenshtat, Z., 2005. Stable sulfur isotope partitioning
during simulated petroleum formation as determined by hydrous pyrolysis of
Ghareb Limestone, Israel. Geochimica et Cosmochimica Acta 69, 5317–5331.

Amrani, A., Sessions, A.L., Adkins, J.F., 2009. Compound-specific δ^{34}S analysis of
volatile organics by coupled GC/multicollector-ICPMS. Analytical Chemistry 81,
9027–9034.

Amrani, A, Sessions, A.L., Tang, Y., Adkins, J.F., Hills, R.J., Moldowan, M.J., Wei, Z.,
2012. The sulfur-isotopic compositions of benzothiophenes and dibenzo-thiophenes

as a proxy for thermochemical sulfate reduction. Geochimica et Cosmochimica Acta 84, 152–164.

Cai, C., Li, K., Anlai, M., Zhang C., Xu, Z., Worden, R.H., Wu, G., Zhang, B., Chen, L., 2009. Distinguishing Cambrian from Upper Ordovician source rocks: Evidence from sulfur isotopes and biomarkers in the Tarim Basin. Organic Geochemistry 40, 755–776.

Cai, C., Zhang, C., Worden, R.H., Wang, T., Li, H., Jiang, L., Huang, S., Zhang, B., 2015. Application of sulfur and carbon isotopes to oil–source rock correlation: A case study from the Tazhong area, Tarim Basin, China. Organic Geochemistry 83–84, 140–152.

Cai, C., Amrani, A., Worden, R.H., Xiao, Q., Wang, T., Gvirtzman, Z., Li, H., Said-Ahmad, W., Lianqi, J., 2016. Sulfur isotopic compositions of individual organosulfur compounds and their genetic links in the Lower Paleozoic petroleum pools of the Tarim Basin, NW China. Geochimica et Cosmochimica Acta 182, 88–108.

Chambers, L.A., Trudinger, P.A., Smith, J.W., Burns, M.S., 1975. Sulfur isotope fractionation during sulfate reduction by dissimilatory sulfate reducing bacteria. Canadian Journal of Microbiology 21, 1602–1607.

Claypool, G.E., Holser, W.T., Kaplan, I.R., Sakai, K., Zak, I., 1980. The age curves of sulfur and oxygen isotopes in marine sulfate and their mutual interpretation. Chemical Geology 28, 199–260.

Dunnington, H.V., 2005. Generation, migration, accumulation, and dissipation of oil in Northern Iraq. Geoarabia 10, 39–84.

Ehrlich, H.L., 1990. Geomicrobiology, Second ed. Marcel Dekker, New York.

Ellis, G.S., Said-Ahmad, W., Lillis, P.G., Shawar, L., Amrani, A., 2017. Effects of thermal maturation and thermochemical sulfate reduction on compound-specific sulfur isotopic compositions of organosulfur compounds in Phosphoria oils from the Bighorn Basin, USA. Organic Geochemistry 103, 63–78.

Engel, M.H., Zumberge, J.E., 2007. Secular change in the stable sulfur isotope composition of crude oils relative to marine sulfates and sulfides. Book of Abstracts, International Meeting of Organic Geochemistry 2007 (Torquay, UK, September 19–24), pp. 523–524.

Faure, G., Mensing, T.M., 2005. Isotopes, Principles and Applications, Third Edition. John Wiley & Sons, Inc., Hoboken, New Jersey.

Gaffney, J.S., Premuzic E.T., Manowitz, B., 1980. On the usefulness of sulfur isotope ratios in crude oil correlations. Geochimica et Cosmochimica Acta 44, 135–139.

Garcia, C.L., Becchi, M., Grenier-Loustalot, M.F., Païsse, O., Szymanski, R., 2002. Analysis of aromatic sulfur compounds in gas oils using GC with sulfur chemiluminescence detection and high-resolution MS. Analytical Chemistry, 74, 3849–3857.

Greenwood, P.F., Amrani, A., Sessions, A., Raven, M.R., Holman, A.I., Dror, G., Grice, K., McCulloch, M.T., Adkins, J.F., 2014. Development and initial biogeochemical applications of compound specific $\delta^{34}S$ analysis. In: Grice, K. (Ed.),

23

RSC Detection Science Series No. 4: Principles and Practice of Analytical Techniques in Geosciences. Royal Society of Chemistry, Oxford.

Greenwood, P.F., Schwark, L., Mohammed, L., Zhu, G., Grice, K., McCulloch, M., 2015. Compound-specific sulfur isotope analysis of oils using GC-MC-ICPMS. Book of Abstracts, International Meeting of Organic Geochemistry 2015 (Prague, Czech Republic, September 13-18) pp 113–114.

Grotheer, H., Greenwood, P.F., McCulloch, M., Böttcher, M.E., Grice, K., 2017. δ^{34}S character of organosulfur compounds in kerogen and bitumen fractions of sedimentary rocks. Organic Geochemistry 110, 60–64.

Gvirtzman, Z., Said-Ahmad, W., Ellis, G.S., Hill, R.J., Moldowan, J.M., Wei, Z., Amrani, A., 2015. Compound-specific sulfur isotope analysis of thiadiamondoids of oils from the Smackover Formation, USA. Geochimica et Cosmochimica Acta 167, 144–161.

Hughes, W.B., Holba, A.G., Dzou, L.I.P., 1995. The ratios of dibenzothiophene to phenanthrene and pristane to phytane as indicators of depositional environment and lithology of petroleum source rocks. Geochimica et Cosmochimica Acta 59, 3581–3598.

Idiz, E.F., Tannenbaum, E., Kaplan, I.R., 1990. Pyrolysis of high-sulfur Monterey kerogens – stable isotope of sulphur, carbon and hydrogen. In: Orr, W.L., White, C.M. (Eds.), Geochemistry of Sulphur in Fossil Fuels, ACS Symposium Series 429. American Chemical Society, pp. 575–591.

Li., S., Amrani, A., Pang, X., Yang, H., Ward, S-A., Zhang, B., Pang, Q., 2015. Origin and quantitative source assessment of deep oils in the Tazhong Uplift, Tarim Basin. Organic Geochemistry 78, 1–22.

Machel, H.G., 1995. Products and distinguishing criteria of bacterial and thermochemical sulfate reduction. Applied Geochemistry 8, 373–389.

Machel, H.G., 2001. Bacterial and thermochemical sulfate reduction in diagenetic settings–old and new insights. Sedimentary Geology 140, 143–175.

Mohialdeen, I.M.J., Hakimi, M.H., 2016. Geochemical characterisation of Tithonian–Berriasian Chia Gara. Organic-rich rocks in northern Iraq with an emphasis on organic matter enrichment and the relationship to the bioproductivity and anoxia conditions. Journal of Asian Earth Sciences 116, 181–197.

Mohialdeen, I.M.J., Hakimi, M.H., Al-Beyati, F.M., 2013. Geochemical and petrographic characterization of Late Jurassic–Early Cretaceous Chia Gara Formation in Northern Iraq: palaeoenvironment and oil-generation potential. Marine Petroleum Geology 43, 166–177.

Mohammed, L.J., 2016. Petroleum System Analysis of the Lower Jurassic-Upper Cretaceous Source and Miocene Reservoirs in the NE of Iraq. Ph.D. thesis, Kiel University.

Mohammed, L.J., Schwark, L., 2013. The upper Jurassic petroleum system of NE Iraq. Book of Abstracts, International Meeting of Organic Geochemistry 2013 (Tenerife, Spain, September 15-20), Vol II, pp. 395–396.

Orr, W.L., 1986. Kerogen/asphaltene/sulphur relationships in sulphur-rich Monterey oils. Organic Geochemistry 10, 499–516.

Postgate, J.R., 1984. The Sulfate-Reducing Bacteria, Second ed. Cambridge University Press, Cambridge.

Rosenberg, Y.O., Meshoulam, A., Said-Ahmad, W., Shawar, L., Dror, G., Reznik, I.J., Feinstein, S., Amrani, A., 2017. Study of thermal maturation processes of sulfur-rich source rock using compound specific sulfur isotopes analysis. Organic Geochemistry 112, 59–74.

Thode, H.G., 1981. Sulfur isotope ratios in petroleum research and exploration: Williston Basin. The American Association of Petroleum Geologists Bulletin 65, 1527–1537.

Thode, H.G, Munster, J., 1970. Sulfur isotope abundances and genetic relations of oil accumulations in Middle East Basin. The American Association of Petroleum Geologists Bulletin 54, 627–637.

Wu, N., Farquhar, J., Strauss, H., 2014. δ^{34}S and Δ^{33}S S records of Paleozoic seawater sulfate based on the analysis of carbonate associated sulfate. Earth and Planetary Science Letters 399, 44–51.

Table Captions

Table 1. List of source rock samples (from well Ajeel-12) and their: (A) molecular and (B) $\delta^{34}S$ data.

Table 2. List of production oils and their measured: (A) molecular and (B) $\delta^{34}S$ data.

Figure Captions

Fig. 1. Jurassic basal Cretaceous stratigraphy of the Arabian Platform; with TOC, HI and T_{max} data from Rock Eval pyrolysis of sediment samples (data from Mohammed and Schwark, 2013).

Fig. 2. Location of major oil fields in study with inset showing geographic map of Iraq.

Fig. 3. Thioaromatic product distributions evident in the *m*/*z* 32 chromatogram from GC–ICPMS analysis of Ajeel oil 4407 (top) and Chia Gara formation rock 4272 (bottom). Separated dimethyl DBT and trimethyl DBT isomers are identified as i, ii, or iii.

Fig. 4. $\delta^{34}S_{OSC}$ profiles of: (A) different production oil fields. i.e., averaged values from all oils (number of oils given in parenthesis) of specific field; (B) three Jambur oils and five Khabbaz oils.

Fig. 5. $\delta^{34}S$ plots of first eluting methyl DBT (4m-) and dimethyl DBT (-i) for the production oils (squares) and rock extracts (circles).

Fig. 6. Plots of: (A) DBT/P vs Pr/Ph for the production oils (left) and rock extracts (right), inferring different depositional environment and lithologies of source rocks (after Hughes et al., 1995); and (B) methyl DBT/methyl P vs DBT/P of production oils, distinguishing oils on basis of their OSC content.

Fig. 7. Plot of δ^{34}S dimethyl DBTi values vs DBT/P ratios for the production oils.

Fig. 8. Average δ^{34}S of selected OSCs from three production oils and two candidate source rocks characterised as having very similar aliphatic biomarker and thioaromatic compositions. The number of oil or rock samples represented by average values are indicated in parenthesis.

Table 1. List of source rock samples (from well Ajeel–12) and their measured molecular (1A) and δ^{34}S (1B) data.

1A:

Well AJ–12 Sample	Formation	Molecular Data				
		Pr/Ph	*Pr/n-C$_{17}$*	*Ph/n-C$_{18}$*	*DBT/P*	*mDBT/mP*
4246	L. Sarmond	0.83	0.31	0.37	0.34	1.91
4271	Chia Gara	0.65	0.22	0.44	1.59	2.02
4272	Chia Gara	0.75	0.21	0.44	1.99	2.43
4350	Chia Gara	0.42	0.24	0.55	1.95	2.34
4360	Chia Gara	1.05	0.31	0.30	1.84	2.29
4312	Gotnia	0.33	0.20	0.38	7.89	9.91
4313	Gotnia	0.40	0.15	0.32	7.74	9.16
6946	Gotnia	0.54	0.22	0.36	1.37	2.55
6947	Gotnia	0.44	0.19	0.33	1.46	2.46
4142	Naokelekan	0.62	0.09	0.14	1.93	3.10
4318	Naokelekan	0.75	0.17	0.26	1.58	3.01
4319	Naokelekan	0.83	0.19	0.28	1.61	3.03
4370	Naokelekan	1.43	0.31	0.25	1.66	3.00
4281	Sargelu	0.72	0.19	0.28	0.82	2.27
4375	Sargelu	0.67	0.19	0.33	1.15	3.06
4377	Sargelu	0.44	0.19	0.32	1.20	2.49
4288	Alan	0.59	0.26	0.37	1.18	2.58
4289	Alan	0.69	0.23	0.34	1.21	4.53

Pr = pristane, Ph = phytane, *n*-C$_{17}$ = *n*-heptadecane, *n*-C$_{18}$ = *n*-octadecane, DBT = dibenzothiophene,

P = phenanthrene, mDBT = methyl dibenzothiophene, mP = methyl phenanthrene

1B:

Well AJ–12 Sample	Formation	δ34S data (‰)										
		mBTi	*mBTii*	*dmBTi*	*dmBTii*	*DBT*	*4mDBT*	*2/3mDBT*	*dmDBTi*	*dmDBTii*	*dmDBTiii*	*tmDBTi*
4246	L. Sarmond	–	–	–	–	–9.7	–12.1	–10.3	–14.6	–12.8	–13.1	
4271	Chia Gara	–2.9	–2.7	–3.6	–4.8	–12.8	–15.1	–14.2	–16.1	–16.6	–15.5	
4272	Chia Gara	–3.0	–4.3	–4.5	–6.8	–11.9	–11.6	–10.6	–12.5	–11.4	–10.8	–11.2
4350	Chia Gara	–	–	–	–	–8.6	–9.9	–10.1	–12.2	–11.7	–11.0	–10.9
4360	Chia Gara	–	–	–	–	–11.9	–11.6	–11.4	–10.5	–10.6	–10.6	–10.7
4312	Gotnia	–	–	–	–	–14.7	–15.5	–13.8	–15.5	–14.5	–13.6	–15.2
4313	Gotnia	–	–	–3.2	–5.9	–13.4	–15.1	–13.8	–14.5	–14.0	–14.0	–13.6
6946	Gotnia	–	–	–	–	–11.3	–14.0	–13.2	–14.8	–14.8	–14.1	
6947	Gotnia	–	–	–	–	–7.4	–11.1	–9.8	–12.6	–11.7	–10.4	–12.0
4142	Naokelekan	–	–	–	–	–17.3	–14.2	–15.6	–15.2	–15.1	–13.5	–15.0
4318	Naokelekan	–5.6	–6.2	–7.6	–9.0	–11.9	–14.3	–13.3	–15.5	–14.1	–13.6	–15.2
4319	Naokelekan	–4.5	–6.4	–7.9	–9.2	–12.2	–16.4	–15.1	–13.7	–12.9	–11.9	–12.6
4370	Naokelekan	–	–	–	–	–15.6	–15.0	–14.2	–15.2	–13.9	–13.6	–13.7
4281	Sargelu	–3.0	–4.3	–6.8	–3.4	–10.0	–12.3	–11.0	–13.6	–12.6	–11.2	–11.3
4375	Sargelu	–4.4	–6.0	–6.5	–7.3	–11.3	–14.0	–13.2	–14.8	–14.8	–14.1	
4377	Sargelu	–	–	–	–	–7.4	–11.1	–9.8	–12.6	–11.7	–10.4	–12.0
4288	Alan	–	–	–4.2	–7.5	–13.7	–16.7	–15.4	–18.4	–17.2	–16.3	
4289	Alan	–	–	–	–	–9.4	–12.9	–9.7	–14.5	–12.9	–10.8	–12.6

mBTi = methyl benzothiophene (isomer i), dmBT = dimethyl benzothiophene, DBT = dibenzothiophene, mBDT = methyl dibenzothiophene, dmDBT = dimethyl dibenzothiophene, tmDBT = trimethyl dibenzothiophene.

Table 2: List of production oils and their measured molecular (2A) and δ^{34}S (2B) data.

2A:

Oil	Oil Field	Molecular Data				
Sample		*Pr/Ph*	*Pr/n-C$_{17}$*	*Ph/n-C$_{18}$*	*DBT/P*	*mDBT/mP*
5404	Jambur	0.92	0.31	0.37	2.66	3.33
5403	Jambur	0.91	0.28	0.34	2.65	3.30
5402	Jambur	0.96	0.29	0.35	2.52	3.30
5401	Hamrin	1.04	0.37	0.40	0.33	0.52
5400	Hamrin	0.98	0.35	0.42	1.75	2.23
4426	Kirkuk	1.01	0.34	0.38	0.36	0.71
4425	Kirkuk	0.87	0.32	0.41	0.41	0.95
4424	Kirkuk	0.86	0.30	0.38	2.14	2.82
4423	Kirkuk	0.90	0.33	0.38	0.96	1.44
4422	Kirkuk	0.89	0.31	0.38	0.67	1.09
4421	Kirkuk	0.89	0.32	0.40	2.22	2.81
4420	Kirkuk	0.94	0.34	0.39	2.17	2.76
4419	Kirkuk	0.92	0.33	0.41	2.21	2.73
4418	Bai Hassan	0.95	0.31	0.36	0.65	0.99
4417	Bai Hassan	0.93	0.31	0.38	0.74	0.89
4416	Bai Hassan	0.88	0.31	0.39	0.76	1.00
4415	Bai Hassan	0.91	0.32	0.39	1.00	1.06
5407	Bai Hassan	0.82	0.27	0.37	0.72	1.24
5405	Bai Hassan	0.83	0.28	0.38	0.44	0.91
4414	Bai Hassan	1.06	0.35	0.36	0.84	1.17
4413	Khabbaz	0.96	0.35	0.41	2.14	2.83
4412	Khabbaz	0.78	0.22	0.32	2.28	3.33
4411	Khabbaz	1.00	0.37	0.42	2.37	2.81
4410	Khabbaz	1.04	0.36	0.39	2.30	2.70
4409	Khabbaz	0.74	0.21	0.33	2.96	3.65
4408	Ajeel	1.03	0.35	0.38	1.67	2.33
4407	Ajeel	1.01	0.39	0.44	1.69	2.06
5406	Baiji	0.86	0.24	0.31	0.89	1.95
6993	Tikrit	0.91	0.28	0.35	0.79	1.56

Pr = pristane, Ph = phytane, n-C_{17} = n-heptadecane, n-C_{18} = n-octadecane, DBT = dibenzothiophene,

P = phenanthrene, mDBT = methyl dibenzothiophene, mP = methyl phenanthrene

2B:

Oil Sample	Oil Field	δ^{34}S data (‰)										
		mBTi	*mBTii*	*dmBTi*	*dmBTii*	*DBT*	*4mDBT*	*2/3mDBT*	*dmDBTi*	*dmDBTii*	*dmDBTiii*	*tmDBTi*
5404	Jambur	0.3	−1.1	−1.4	−1.6	−2.5	−5.1	−4.4	−6.4	−6.2	−5.2	−7.4
5403	Jambur	1	−0.3	−1	−0.9	−3.3	−5.1	−3.3	−6.4	−5.5	−4.4	−8.1
5402	Jambur	3.4	−0.3	1.8	−0.5	−3.3	−5.1	−3.9	−7.2	−3.4	−4.7	−7.1
5401	Hamrin	−0.5	−2.5	−2.4	−3.4	−5.1	−4.7	−4.9	−6.7	−7.4	−7.2	−7.4
5400	Hamrin	−1.8	−3.2	−4.8	−4.1	−4.8	−5.1	−4.5	−6	−6.6	−6.6	−6.7
4426	Kirkuk	1.1	−0.5	−0.7	−1.4	−4.4	−5.1	−4.7	−7	−6.7	−6.2	−8.7
4425	Kirkuk	0.2	−1	−1.5	−2.6	−4.5	−6.5	−7.1	−7.4	−8.1	−7.5	−8
4424	Kirkuk	−2.4	−2.5	−4.9	−3.2	−5.3	−7.4	−5.3	−7.9	−6.6	−6.8	−8
4423	Kirkuk	−	−	−	−	−6.9	−7.3	−5.3	−7.9	−6.5	−5.5	−8.7
4422	Kirkuk	−	−	−	−	−7.9	−7.2	−6.9	−8.7	−7.7	−7.1	−9.8
4421	Kirkuk	−1.6	−2	−3.4	−3	−5.4	−6.3	−5.1	−7.3	−6.3	−5.3	−8.2
4420	Kirkuk	−0.8	−1	−3	−1.7	−4.8	−6.5	−3.8	−7.3	−5.8	−4.9	−8.4
4419	Kirkuk	−1.4	−1.5	−3.1	−2.5	−5.7	−6.4	−4.9	−7.7	−6.3	−5.2	−8
4418	Bai Hassan	−0.7	−2.2	−2.5	−2.8	−5	−6.7	−6.1	−8.3	−7.4	−7	−8.4
4417	Bai Hassan	−2.4	−3	−3.3	−3.5	−5.8	−7	−6.1	−8.2	−6.6	−7.8	−9.1
4416	Bai Hass	0.2	−1	−1.9	−2.2	−6.6	−6.5	−6.5	−7.5	−8.1	−7.7	−8.3

32

	an										
4415	Bai Hassan	–0.6	–1.6	–2.4	–2.8	–5.8	–7.1	–6.9	–7.8	–8.3	–7.7	–9.2
5407	Bai Hassan	–1.6	–2.1	–3.3	–3	–5.8	–7.9	–7.4	–9.3	–7.3	–7.4	–8.1
5405	Bai Hassan	–0.8	–2.2	–2.6	–3.1	–7	–6.4	–5.7	–7.1	–8.1	–8.2	–9.2
4414	Bai Hassan	–0.9	–1.4	–2.2	–2.6	–5.6	–6.5	–5.7	–7	–7.7	–6.8	–9.3
4413	Khabbaz	–0.4	–2.6	–3	–3.9	–6.7	–6.9	–7	–8	–8	–8.5	–8.6
4412	Khabbaz	0.4	–2.6	–2.5	–2	–3.4	–4.6	–4.4	–7.3	–7.5	–7.1	–10
4411	Khabbaz	1.7	–1.6	–1.1	–3	–5.8	–9.4	–8.8	–11	–10.9	–10	–11.6
4410	Khabbaz	–5.7	–5.3	–5.8	–5.5	–8.4	–10.5	–10.1	–11.2	–10.5	–10	–10.9
4409	Khabbaz	–1	–2.7	–2.6	–3.9	–6.6	–8.6	–6.6	–9.8	–8.4	–7.1	–10.6
4408	Ajeel	–1.4	–0.5	–3.5	–2.1	–4.7	–5.6	–3.1	–6.1	–4.9	–3.1	–8.1
4407	Ajeel	1	0.7	0	–1.3	–2.9	–4.8	–3	–6.3	–5	–4	–7.4
5406	Baiji	–0.5	–1	–2.4	–2.8	–6.9	–8.6	–5.9	–10	–7.1	–6.4	–8.9
6993	Tikrit	2.7	2.1	0.8	0.7	–2.3	–4	–2.5	–5.5	–4.7	–5	–6

mBTi = methyl benzothiophene (isomer i), dmBT = dimethyl benzothiophene, DBT = dibenzothiophene, mBDT = methyl dibenzothiophene, dmDBT = dimethyl dibenzothiophene, tmDBT = trimethyl dibenzothiophene.

Highlights

- Organic sulfur compounds (OSCs) were studied in Kurdistan oils and source rocks
- $\delta^{34}S$ values indicate separate oil and rock groups ($> 2‰$ difference).
- OSCs from rocks were 2–4‰ depleted than OSCs in oils
- Related oils and rocks were inferred from relative ^{34}S enrichment or depletion.